**Electronic Supplementary Information for**

Atomically dispersed Cu and Fe on N-doped carbon materials for CO$_2$ electroreduction: Insight into the curvature effect on activity and selectivity

Yue Zhang, Lei Fang, and Zexing Cao*

State Key Laboratory of Physical Chemistry of Solid Surfaces and Fujian Provincial Key Laboratory of Theoretical and Computational Chemistry, College of Chemistry and Chemical Engineering, Xiamen University, Xiamen 360015, China
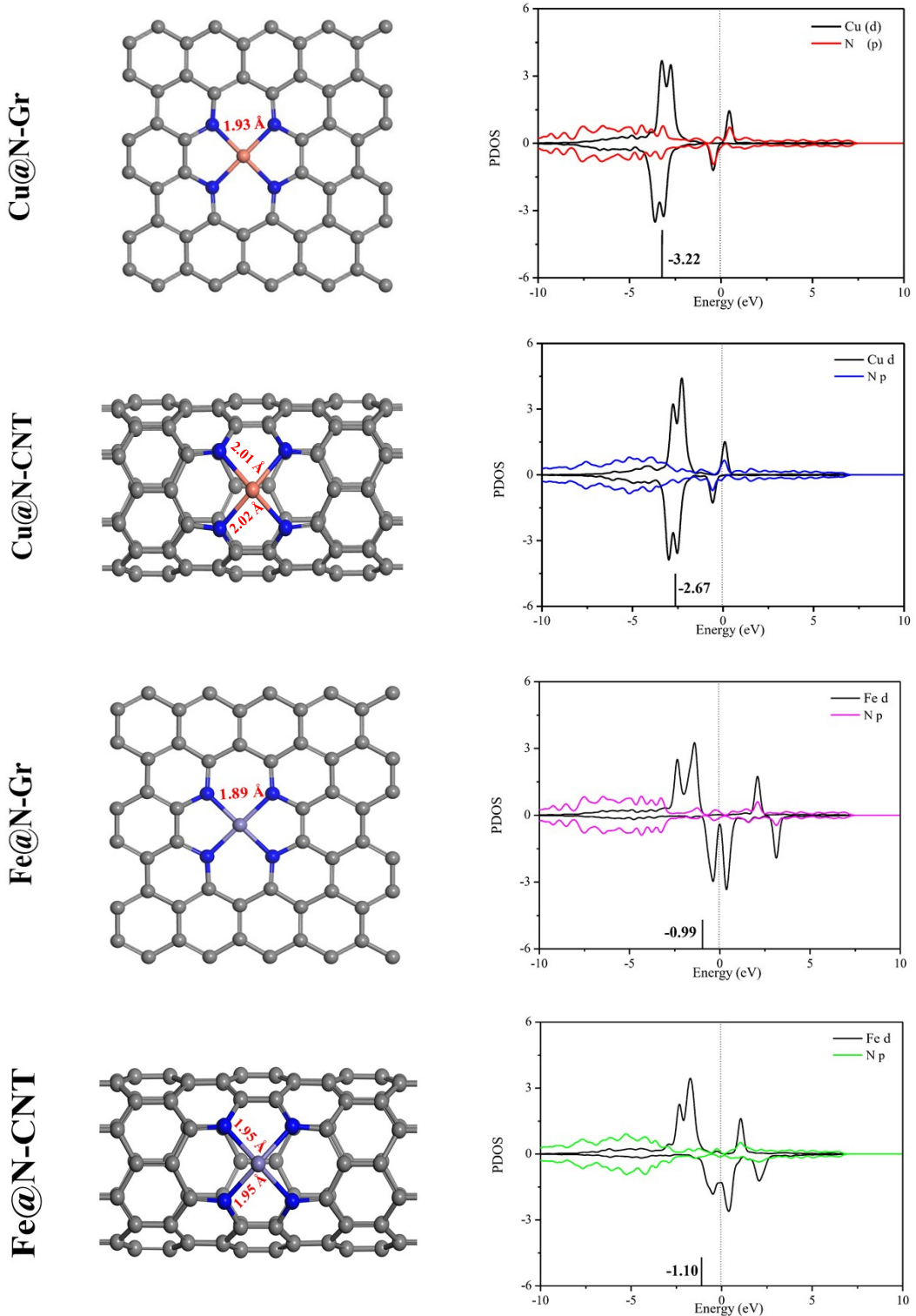
**Fig. S1.** Optimized structures and projected density of states (PDOS) of Cu@N-Gr, Cu@N-CNT, Fe@N-Gr and Fe@N-CNT, where the corresponding d-band centers (ε_d) of -3.22, -2.67, -0.99 and -1.10 eV are presented.
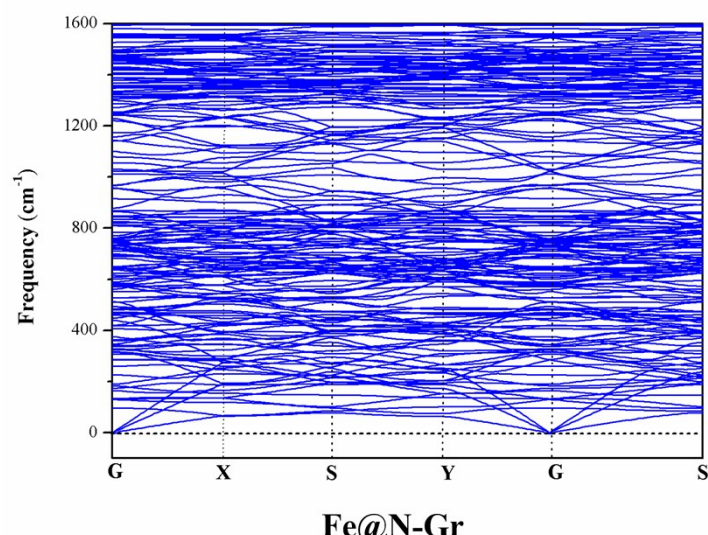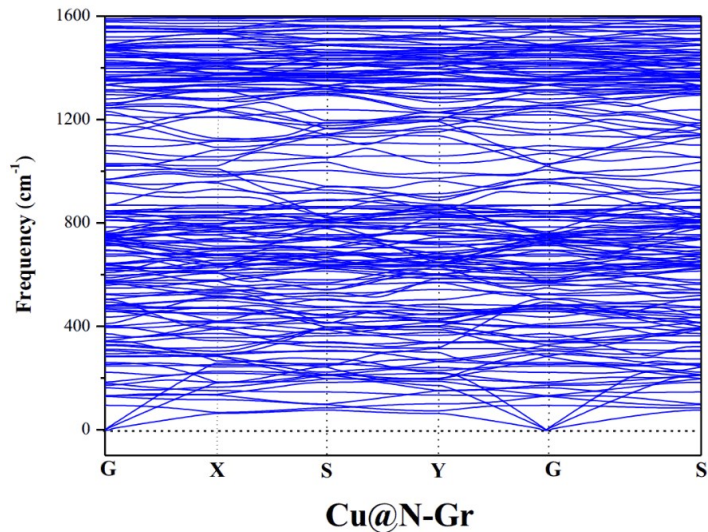
Fig. S2 The phonon spectra of Cu@N-Gr and Fe@N-Gr, where *G*(0, 0, 0), *X*(1/2, 0, 0), *S*(1/2, 0, 0), and *Y*(0, 1/2, 0) are the high-symmetric points in the first Brillouin region.
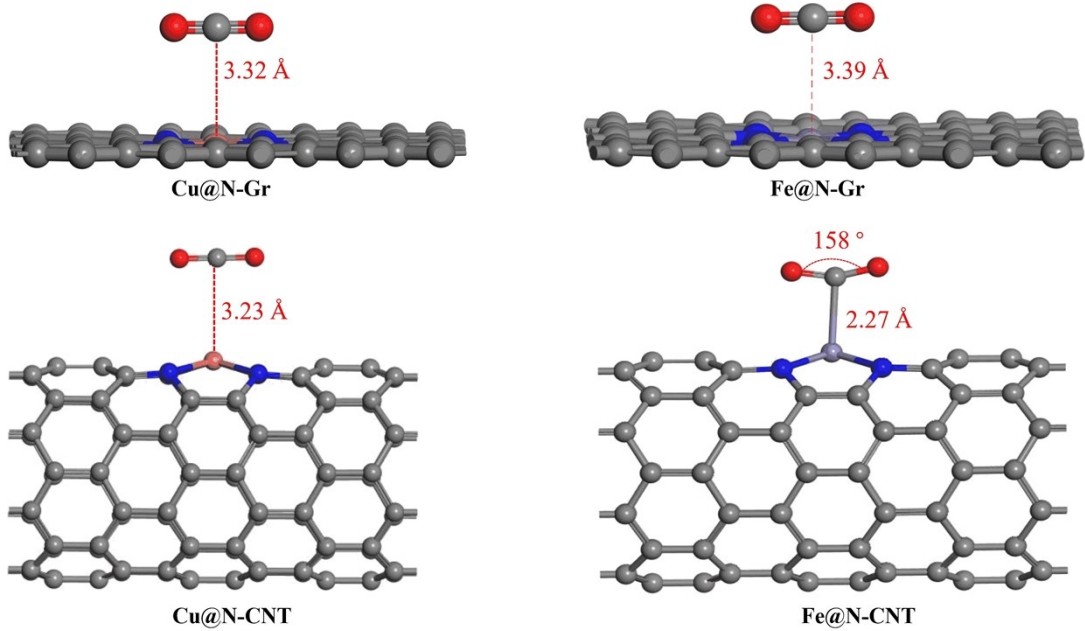
Fig. S3. The adsorption configuration of CO_2 on Cu@N-Gr, Cu@N-CNT, Fe@N-Gr, and Fe@N-CNT.
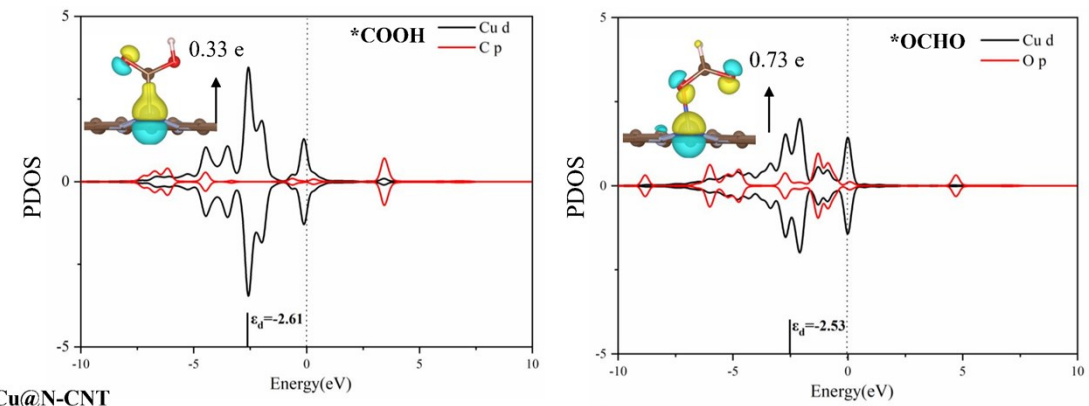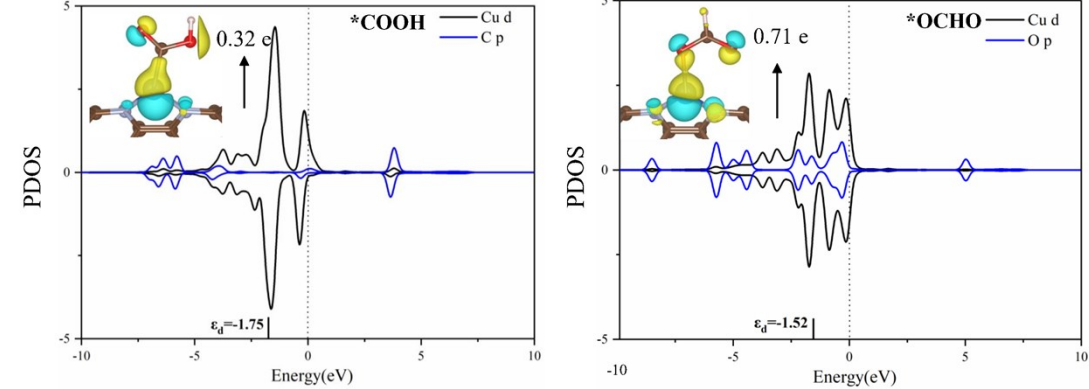
Fig. S4. The PDOS and differential charge density of COOH/OCHO species adsorbed on Cu@N-Gr and Cu@N-CNT.
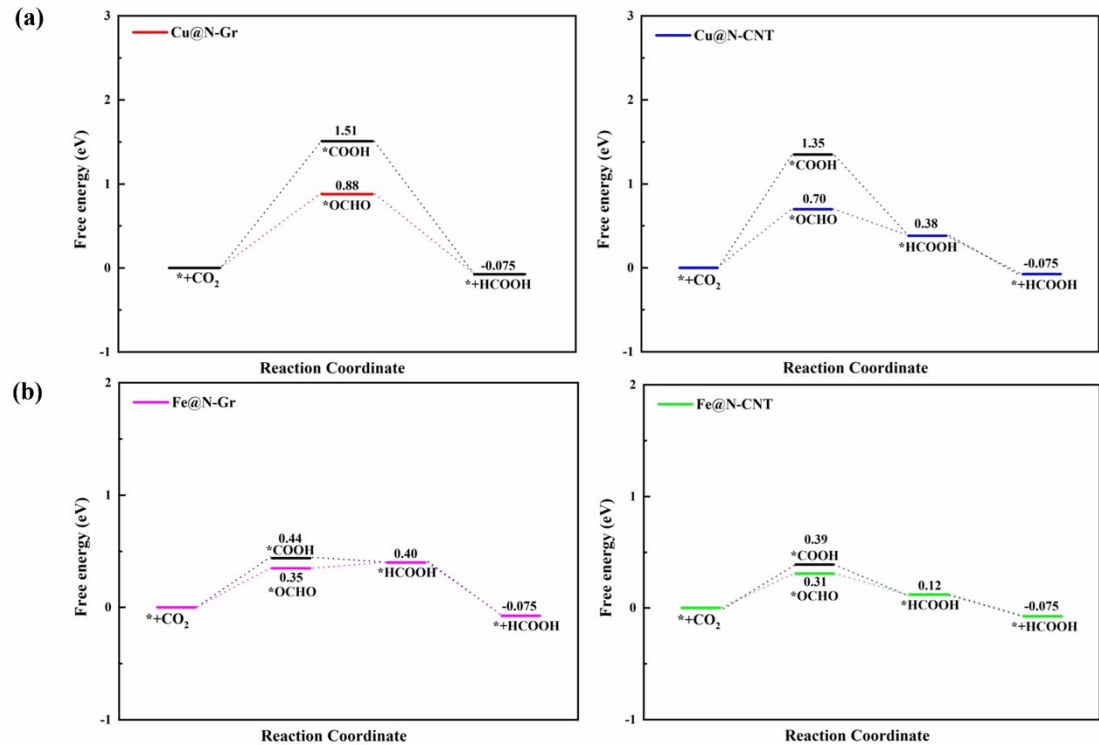
Fig. S5. Different reaction pathways and predicted relative free energy diagrams of CO_2ER to HCOOH on (a) Cu nanostructures and (b) Fe nanostructures, where red, blue, pink and green represent the low-energy pathways on Cu@N-Gr, Cu@N-CNT, Fe@N-Gr and Fe@N-CNT, and the other routes are highlighted in black.
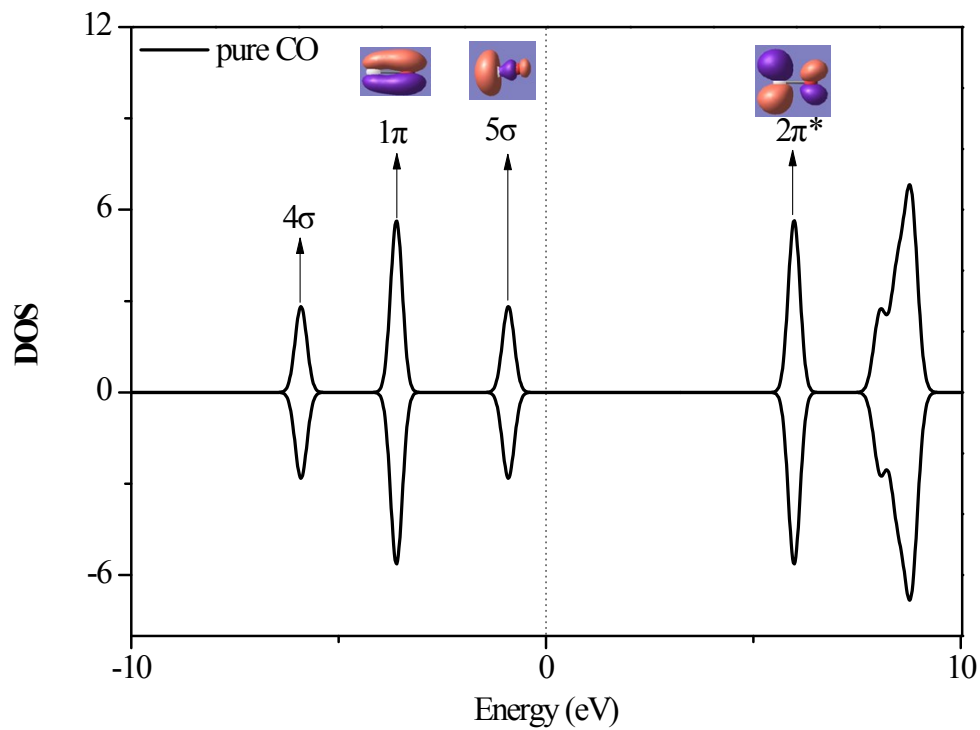
Fig. S6. Calculated density of states (DOS) of the isolated CO.
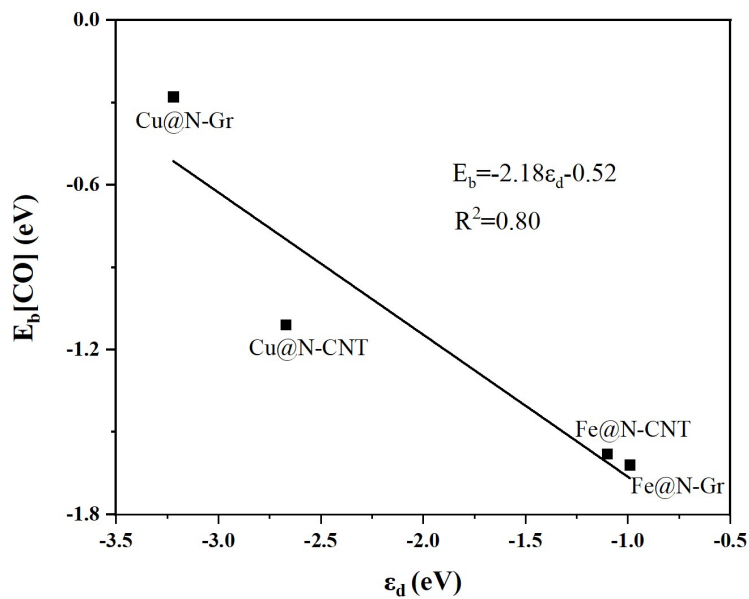
Fig. S7. Linear correlation between the *CO binding energy (E_b) and ε_d of metal atoms in Cu@N-Gr, Cu@N-CNT, Fe@N-Gr and Fe@N-CNT.
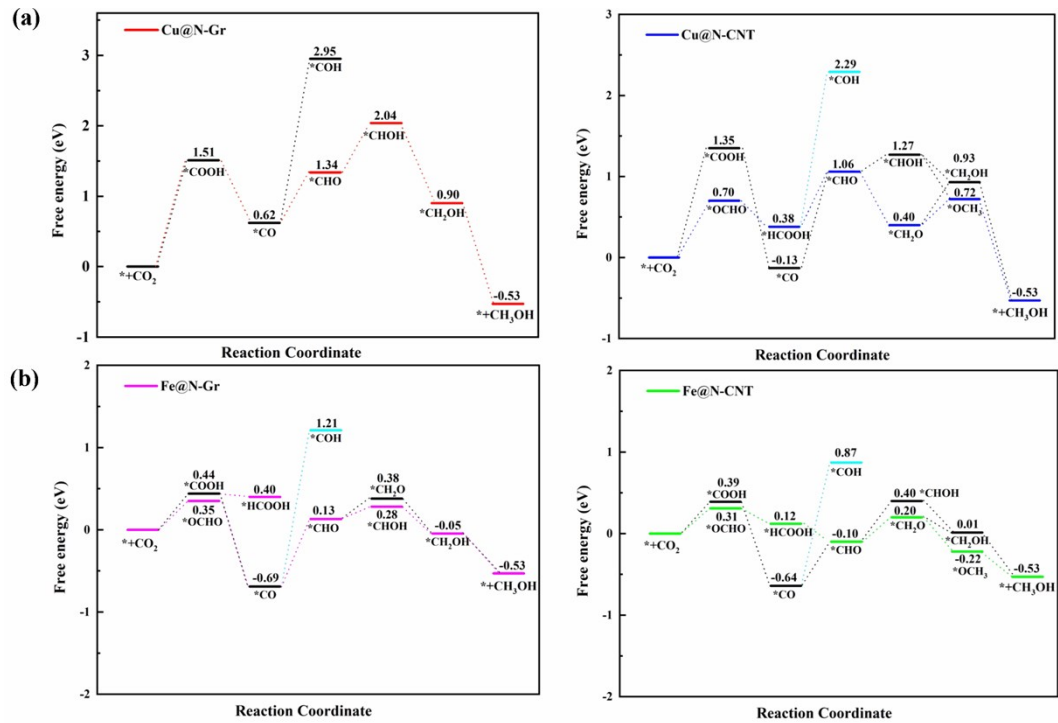
Fig. S8. Different reaction pathways and predicted relative free energy diagrams of CO$_2$ER to CH$_3$OH.
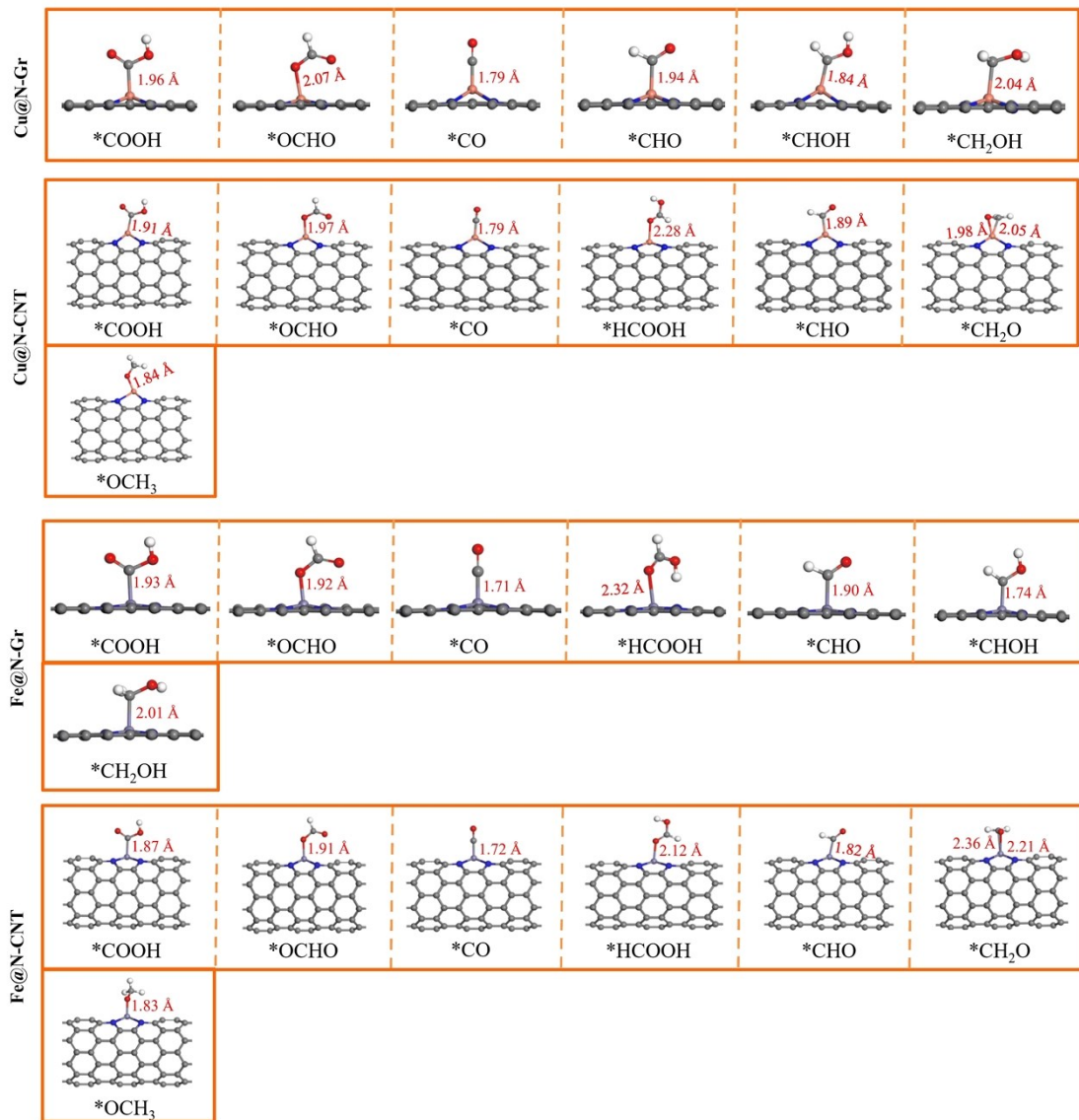
Fig. S9. The optimized configurations of main species involved in CO_2ER on Cu@N-Gr, Cu@N-CNT, Fe@N-CNT and Cu@N-CNT.
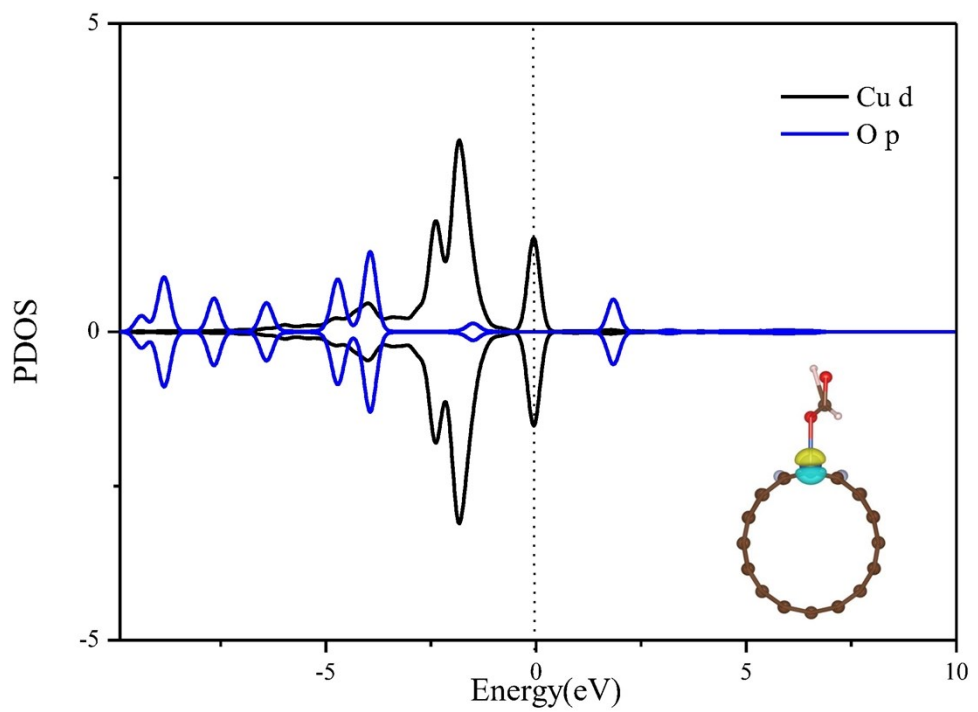
Fig. S10. The PDOS and differential charge density of HCOOH specie adsorbed on Cu@N-CNT.
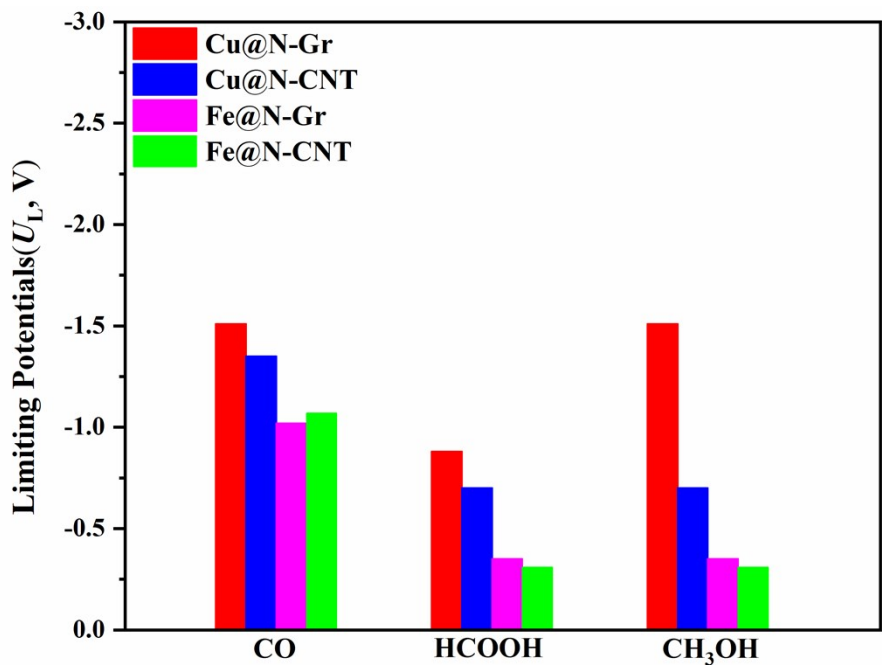
Fig. S11. The limiting potential diagram of generating CO, HCOOH, and CH$_3$OH on Cu@N-Gr, Cu@N-CNT, Fe@N-Gr and Fe@N-CNT in water solution.

Table S1. Electronic energy (E_{ele}), thermodynamic energy corrections (E_{ZPE}, TS, $\int C_p \, dT$) and Gibbs free energy (G) of involved gaseous species (in eV).

Species	E_{ele}	E_{ZPE}	TS	$\int C_p \, dT$	G^a
CO_2	-22.95	0.31	0.66	0.10	-23.21
CO	-14.77	0.13	0.61	0.09	-15.16
H_2O	-14.22	0.57	0.58	0.10	-14.14
H_2	-6.77	0.27	0.40	0.09	-6.81
HCOOH	-29.89	0.89	0.77	0.11	-29.66
CH_3OH	-30.22	1.35	0.74	0.11	-29.50

[a] $G = E_{ele} + E_{ZPE} + \int C_p dT - TS$, where E_{ZPE}, $\int C_p dT$, TS are the zero-point energy, enthalpy change contributed by molecular vibration from 0 to 298 K, and entropy correction, respectively.

Table S2. CO_2ER reduction pathways and free energy changes (ΔG/eV) on Cu@N-Gr, Cu@N-CNT, Fe@N-Gr and Fe@N-CNT, where ΔG_1 and ΔG_2 are the free energy changes in gas phase and water solvent, respectively.

Elementary steps	Cu@N-Gr		Cu@N-CNT		Fe@N-Gr		Fe@N-CNT	
	ΔG_1	ΔG_2	ΔG_1	ΔG_2	ΔG_1	ΔG_2	ΔG_1	ΔG_2
* + CO_2 + H^+ + e^- → *COOH	1.66	1.51	1.54	1.35	0.57	0.44	0.54	0.39
* + CO_2 + H^+ + e^- → *OCHO	0.90	0.60	0.71	0.34	0.16	0.05	-0.00	-0.12
*COOH + H^+ + e^- → *CO + H_2O	-0.80	-0.88	-1.48	-1.48	-1.03	-1.13	-0.96	-1.02
*CO → * + CO	-0.22	-0.20	0.57	0.56	1.09	1.12	1.07	1.06
*COOH + H^+ + e^- → * + HCOOH	-1.51	-1.58	—	—	—	—	—	—
*OCHO + H^+ + e^- → * + HCOOH	-0.96	-0.92	—	—	—	—	—	—
*COOH + H^+ + e^- → *HCOOH	—	—	-0.98	-0.98	-0.17	-0.04	-0.24	-0.27
*OCHO + H^+ + e^- → *HCOOH	—	—	-0.49	-0.32	-0.04	0.05	-0.09	-0.19
*HCOOH → * + HCOOH	—	—	-0.42	-0.45	-0.26	-0.47	-0.15	-0.19
*CO + H^+ + e^- → *CHO	0.79	0.71	1.28	1.19	0.90	0.82	0.61	0.54
*CO + H^+ + e^- → *COH	2.72	2.33	2.80	2.41	2.17	1.90	1.82	1.51
*HCOOH + H^+ + e^- →*CHO + H_2O	—	—	0.78	0.69	0.04	-0.27	-0.12	-0.22
*CHO + H^+ + e^- → *CHOH	0.99	0.70	0.43	0.20	0.29	0.15	0.68	0.49
*CHO + H^+ + e^- → *CH_2O	—	—	-0.64	-0.66	0.23	0.25	0.30	0.30
*CHOH + H^+ + e^- → *CH_2OH	-1.33	-1.14	-0.46	-0.33	-0.42	-0.32	-0.49	-0.38
*CH_2O + H^+ + e^- → *CH_2OH	—	—	0.60	0.53	-0.36	-0.43	-0.11	-0.19
*CH_2O + H^+ + e^- → *OCH_3	—	—	0.36	0.32	-0.52	-0.50	-0.46	-0.42
*CH_2OH + H^+ + e^- → * + CH_3OH	-1.44	-1.43	-1.44	-1.47	-0.45	-0.49	-0.50	-0.55
*OCH_3 + H^+ + e^- → *+ CH_3OH	—	—	-1.20	-1.26	-0.29	-0.42	-0.15	-0.32

Table S3. Solvation energies (ΔE_{sol}) of the main reaction intermediates on Cu@N-Gr, Cu@N-CNT, Fe@N-Gr and Fe@N-CNT. ΔE_{sol} is derived from the equation: $\Delta E_{sol} = E_{sol} - E_{ele}$, where E_{ele} and E_{sol} are the electronic energy of intermediates in gas phase and aqueous solvent, respectively.

Intermediates	Cu@N-Gr			Cu@N-CNT		
	E_{ele}	E_{sol}	ΔE_{sol}	E_{ele}	E_{sol}	ΔE_{sol}
*COOH	-560.23	-560.38	-0.15	-876.64	-876.81	-0.17
*OCHO	-560.70	-560.98	-0.28	-877.06	-877.39	-0.33
*CO	-549.87	-549.79	0.08	-866.94	-866.79	0.15
*CHO	-552.72	-552.71	0.01	-869.26	-869.20	0.06
*COH	-550.80	-551.11	-0.31	-867.73	-867.97	-0.25
*CHOH	-555.48	-555.76	-0.29	-872.58	-872.75	-0.17
*CH$_2$O	—	—	—	-873.59	-873.56	0.03
*CH$_2$OH	-560.30	-560.39	-0.10	-876.73	-876.76	-0.03
*OCH$_3$	—	—	—	-876.95	-876.95	-0.00

Intermediates	Fe@N-Gr			Fe@N-CNT		
	E_{ele}	E_{sol}	ΔE_{sol}	E_{ele}	E_{sol}	ΔE_{sol}
*COOH	-566.72	-566.87	-0.15	-882.71	-882.86	-0.15
*OCHO	-566.79	-566.90	-0.11	-882.81	-882.89	-0.08
*CO	-556.55	-556.49	0.06	-872.44	-872.34	0.11
*CHO	-559.30	-559.32	-0.02	-875.47	-875.43	0.04
*COH	-558.06	-558.27	-0.21	-874.31	-874.52	-0.21
*CHOH	-562.73	-562.90	-0.17	-878.56	-878.71	-0.15
*CH$_2$O	-562.81	-562.81	0.01	-878.90	-878.87	0.04
*CH$_2$OH	-566.84	-566.91	-0.07	-882.73	-882.77	-0.04
*OCH$_3$	-566.99	-566.97	0.03	-883.07	-882.99	0.08